International Journal of Medical Microbiology 309 (2019) 54–65

Contents lists available at ScienceDirect

International Journal of Medical Microbiology

journal homepage: www.elsevier.com/locate/ijmm

A versatile remote control system for functional expression of bacterial virulence genes based on the *tetA* promoter

Marc Schulte[1], Torsten Sterzenbach[1], Katarzyna Miskiewicz, Laura Elpers, Michael Hensel*, Nicole Hansmeier*

Abteilung Mikrobiologie, Fachbereich Biologie/Chemie, Universität Osnabrück, Barbarastr. 11, 49076, Osnabrück, Germany

ARTICLE INFO

Keywords:
Tet repressor
Heterologous expression system
Type III secretion system
Fimbrial adhesins
Autotransporter adhesins

ABSTRACT

The expression of bacterial virulence factors is controlled in response to host or environmental factors and most virulence genes are not expressed under laboratory conditions. Investigations of molecular structures and cellular functions of bacterial virulence factors demand systems for experimentally controlled expression. We describe a simple and robust system that is based on the *tetA* promoter and the cognate repressor TetR. Expression under control of P_{tetA} can be induced by non-antibiotic derivatives of tetracycline such as anhydrotetracycline (AHT). Tet-on expression cassettes can be used to replace native promoters of chromosomal genes or operons of interest. Tet-on plasmids allow episomal expression in homologous or heterologous host organisms. We demonstrate the application of Tet-on systems for the controlled induction of flagella assembly and motility, and for surface expression of adhesins of the chaperone/usher family of enteropathogenic *Escherichia coli* and autotransporter adhesins of *Yersinia enterocolitica* in *Salmonella enterica* and *E. coli*. Since inducer AHT can easily cross bacterial envelopes and mammalian cell membranes, the system can also be applied to control virulence genes in intracellular bacteria. We demonstrate the controlled synthesis, translocation and function of effector proteins of the type III secretion system of intracellular *S. enterica*.

1. Introduction

Bacterial pathogens employ a wide range of strategies in order to survive, multiply, and disseminate within hosts and the environment. Central for bacterial pathogenesis are predominantly proteinaceous virulence determinants, which are secreted to the bacterial cell surface or released into the external environment. Although these determinants are structurally diverse, they may be functionally categorized as factors involved in adherence (i.e. fimbria, pili), invasion (i.e. invasin, internalin), immune evasion (i.e. capsule), life inside host cells (i.e. effector proteins) or host cell disintegration (i.e. toxin). Deciphering their structure, function and interaction partners are not only key steps to understand pathogenicity, but also to design new vaccines and targets for new antimicrobials, especially in times of increasing antibiotic resistance (reviewed in Andersson and Hughes, 2010).

However, a major hurdle in studying virulence determinants is their tight regulation, and suitable conditions for their expression in laboratory cultures are either unknown or too complex to mimic. For instance, the food-borne pathogen *Salmonella enterica* serovar Typhimurium (STM) encodes twelve chaperone-usher fimbriae, of which only Type 1 fimbriae are readily expressed under laboratory conditions, whereas all of them are present in the bovine intestines (reviewed in Humphries et al., 2003). Another example are effector proteins of type III or type IV secretion systems (T3SS, T4SS). A wide range of pathogens of plants or animals produce a large spectrum of these functionally highly diverse proteins, which manipulate various host processes and enable the pathogen to establish their virulence. For instance the human pathogen *Legionella pneumophila* encodes more than 250 different effectors (Burstein et al., 2009), 40–60 are present in pathogenic *Escherichia coli* such as EHEC (Tobe et al., 2006), and STM injects a cocktail of more than 60 effector proteins inside the host cytoplasm via two distinct T3SS (Malik-Kale et al., 2011). Although their importance is evident, conditions for *in vitro* expression are often unknown. Furthermore, *in vivo* concentrations of effectors are often low, restricting their functional characterization.

To overcome these obstacles, ectopic and tunable expression systems are the preferred choice for the production of virulence factors in a controlled manner. Various expression systems for controlled

* Corresponding authors.
E-mail addresses: Michael.Hensel@biologie.uni-osnabrueck.de (M. Hensel), Nicole.Hansmeier@biologie.uni-osnabrueck.de, nicole.hansmeier@uregina.ca (N. Hansmeier).
[1] Equal contribution.

https://doi.org/10.1016/j.ijmm.2018.11.001
Received 26 July 2018; Received in revised form 21 October 2018; Accepted 14 November 2018

expression of bacterial genes are available. These systems, however, are mainly optimized for production of recombinant proteins by bacterial strains. One of the most commonly used and therefore best studied systems for recombinant protein expression is the isopropyl β-D-1-thiogalactopyranoside (IPTG)-inducible *lac* system in its natural host *E. coli* (Rosano and Ceccarelli, 2014). It is based on the lactose (*lac*) operon of *E. coli* and protein production can be controlled in a dose-dependent manner with the non-metabolizable molecular mimetic of allolactose (IPTG). While the use of the IPTG system for conditional expression has been established in diverse species (Leclerc et al., 2016; Ravishankar et al., 2015; Rosano and Ceccarelli, 2014), the system showed some limitations in mammalian cell cultures. For instance, the activation of the *lac*-based system in the epithelial model cell line HeLa seems to be lacking and only moderate induction rates were reached (Gossen and Bujard, 1992).

We recently established a tetracycline-inducible (Tet-on) expression system for the analyses of the adhesiome of STM in heterologous host *E. coli* ORN172 (Hansmeier et al., 2017). Tetracycline resistance gene *tetA*, cognate promoter $P_{tetA,}$ and repressor *tetR* are well-studied elements for generation of expression cassettes (reviewed in Berens and Hillen, 2004; Gossen et al., 1994). Tet-on and Tet-off systems have already been widely used in applications ranging from bacteria to mammalian organisms. Studies from Gossen and Bujard (1992) showed its suitability for the mammalian system. Compared to IPTG-inducible systems, this system is activated by addition of very low amounts of AHT, a tetracycline derivate without antibiotic activity and high binding specificity (Mossman, 1983; Oliva et al., 1992).

In this study, we deployed the Tet-on system for the expression of the flagellum and a spectrum of virulence factors including adhesins, invasins, and T3SS-translocated effector proteins from various pathogens, as well as in the mammalian model system HeLa.

2. Materials and methods

2.1. Construction of strains and plasmids

Salmonella enterica serovar Typhimurium (STM) strain NCTC 12023 was used as wild-type (WT) strain and isogenic mutant strains were used in this study. *E. coli* NEBα was used as cloning strain, and *E. coli* ORN172 was used for functional expression of heterologous genes. Mutant strains of STM were generated by λ Red-mediated recombination as previously described (Chakravortty et al., 2002). Bacterial strains and plasmids used in this study are listed in Table S 1. Cultivation of pathogenic and genetically modified bacteria was performed under appropriate biosafety conditions (BL2 for STM, and EC expressing *Yersinia* spp. or EHEC virulence factors).

Template vector p3773, and plasmids p4390 and p4396 for expression of Pef or Stf fimbriae, respectively, were described previously (Hansmeier et al., 2017). The genes encoding YadA and Inv were amplified from genomic DNA of *Y. enterocolitica* harboring virulence plasmid pYV. The operon encoding for Ecp fimbriae (*ecpRABCDE*) was amplified from genomic DNA of *E. coli* O157:H7 (Sakai). Plasmids for Tet-on expression were generated by Gibson assembly (GA) according to manufacturer's instructions (NEB) using p4392 (Hansmeier et al., 2017) as vector by replacing the *fimAICDHF* operon by genes or operons of interest. Oligonucleotides for mutagenesis and GA are listed in Table S 2.

2.2. Cultivation of bacterial strains and induction by AHT

Bacterial strains and cell lines used in this study are listed in Table S 1. Unless otherwise stated, bacteria were routinely grown aerobically in lysogeny broth (LB) (10 g Bacto tryptone, 5 g Bacto yeast extract, 10 g NaCl per liter) or on LB agar plates (LB containing 1.5% Difco agar). If required for the selection of plasmids or chromosomal markers, carbenicillin or kanamycin were added at 50 µg/ml. HeLa (ATCC No. CCL-2) was maintained in DMEM containing 4.5 g/l glucose, 4 mM L-glutamine, sodium pyruvate (Biochrom) and 10% iFCS at 37 °C in an atmosphere containing 5% CO_2 and 90% humidity.

Anhydrotetracycline (AHT) was obtained from Fluka Sigma-Adrich. Stock solutions of 200 µg/ml in dimethylformamide (DMF) were stored in aliquots in the dark at −20 °C. AHT-containing culture media were freshly prepared, or aliquots of AHT were added directly to cultures.

For induction of expression of P_{tetA}-controlled genes or operons, overnight cultures of respective strains were diluted 1:31 in fresh medium with or without AHT and incubated for 3.5 h in a roller drum (New Brunswick), unless otherwise noted.

2.3. Western blotting and immunostaining

Western blotting was performed as described in Hansmeier et al. (2017). Briefly, 1.5×10^{10} bacteria/ml were pelleted and boiled in SDS-PAGE loading buffer containing 0.1% glycine/HCl, pH 2.2 for 5 min. 10 µl lysates were separated on SDS-PAGE with 8–14 % polyacrylamide (depending on the size of the target protein) and transferred onto 0.22 or 0.45 µm nitrocellulose membrane using a semi-dry electrophoretic transfer unit (BioRad). Blots were incubated with respective specific antiserum in indicated dilutions (Table S3), and detected with secondary anti IgG antibody conjugated to horseradish peroxidase and an ECL detection kit (Pierce). Blots were visualized with a Chemidoc imaging system (BioRad).

Immunostaining was performed as described before (Vorwerk et al., 2015). Briefly, infected HeLa cells infected at a multiplicity of infection (MOI) of 75 were fixed with 3% paraformaldehyde (PFA) at indicated time points post infection (p.i.), washed with PBS and incubated for 30 min in blocking solution (2% goat serum, 2% BSA and 0.1% saponin in PBS) before incubated with anti-M45 or anti-HA as primary antibody and matching secondary antibody (Table S3) for 1 h at RT.

2.4. Flow cytometry

Surface expression was analyzed by flow cytometry using a FACSCalibur (Becton Dickinson) instrument. 6×10^8 bacteria were washed with PBS, fixed for 20 min in 3% PFA, before stained with specific antiserum or antibodies as indicated in Table S 3, and labeled with secondary goat anti rabbit IgG antibody coupled to Alexa-Fluor488. Data were analyzed using FCS Express (De Novo Software). A mutant strain devoid of the respective virulence factor was always used as a negative control for gating.

2.5. Infection of HeLa cells

HeLa cells were infected with 3.5 h subcultures of *Salmonella* with a MOI of 75. Infection was allowed to proceed for further 25 min at 37 °C in an atmosphere of 5% CO_2. Subsequently, cells were washed thrice with warm PBS and incubated with medium containing 100 µg/ml gentamicin (AppliChem) to kill non-invaded bacteria for 1 h. Finally, the medium was replaced by medium containing 10 µg/ml gentamicin for the rest of the experiment.

2.6. Visualization by atomic force microscopy (AFM) and transmission electron microscopy (TEM)

AFM measurements were performed using the NanoWizard II AFM system (JPK Instruments AG, Berlin, Germany) in soft contact mode with silicon nitride AFM probes (nominal force constant: 0.06 N/m; SiNi, Budget Sensors, Wetzlar, Germany) and a scan rate of 1 Hz. TEM analysis was conducted using a Zeiss 902 system operating at 50 keV for samples without negative staining. High-resolution analysis and photographs were gained at the negatively stained samples using the Libra 120 TEM (Zeiss) operating at 120 keV and equipped with the Omega energy filter and 2000 × 2000 pixel digital camera (Troendle). Samples

for AFM and TEM were prepared as described before (Hansmeier et al., 2017). Per subject, three biological replicates were imaged with an image resolution of 512 × 512 pixels. Representative images are displayed. AFM images were XY tilt corrected, polynomial-fitted and unsharpened mask filtered to remove noise using JPK data processing software (JPK Instruments AG). TEM micrographs were adjusted for brightness and contrast enhanced using ImageJ or Photoshop software when necessary.

2.7. Confocal laser scanning microscopy (CLSM)

Before live cell imaging, medium was replaced by Minimal Essential Medium (MEM) with Earle's salts, without $NaHCO_3$, L-glutamine and phenol red (BioChrom) but supplemented with 30 mM HEPES, pH 7.4. Fluorescence imaging was mainly performed using the Leica SP5 confocal laser-scanning microscope (CLSM) with live cell periphery, equipped with an incubation chamber maintaining 37 °C and humidity. Objectives 10x (HC PL FL 10x, NA 0.3), 20x (HC PL APO CS 20x, NA 0.7), 40x (HCX PL APO CS 40x, NA 1.25–0.75) and 100x objective (HCX PL APO CS 100x, NA 1.4–0.7) were used and the polychromic mirror TD 488/543/633 for the three channels GFP/ RFP/ BF (Leica, Wetzlar, Germany). The LAS AF software (Leica, Wetzlar, Germany) was used for setting adjustment, image acquisition and image processing. For live cell experiments, the Zeiss Cell Observer microscope with Yokogawa Spinning Disc Unit CSU-X1a, Evolve EMCCD camera (Photometrics, USA) and live cell periphery, equipped with an Alpha Plan-Apochromat 63x (NA 1.46) oil immersion objective (Zeiss) was used. Images were acquired with the following filter combinations: mTurquoise2 with BP 485/30, GFP with BP 525/50, mCherry with LP 580 and processed by the ZEN2012 (Zeiss) software. Scale bars for all acquired images were added with Photoshop CS6 (Adobe).

2.8. Bioinformatics analyses

Statistical analysis was performed by a One-way Analysis of Variance (ANOVA) using SigmaPlot 13.0.

3. Results

3.1. The Tet-on expression system

We established a tetracycline-inducible expression system for controlled expression of adhesins in non-fimbriated *E. coli* strain ORN172 (Hansmeier et al., 2017). Repressor TetR binds to the operator in the *tetA* promoter and represses expression of *tetA*. If tetracycline, inactivated tetracycline, or non-antibiotic derivatives such as anhydrotetracycline (AHT) are present in the cell, these compounds bind to TetR and induce conformational changes that results in release of operator binding and derepression of *tetA* expression. Tetracycline and derivatives are small, membrane-permeable compounds that enter cells without need for specific transport, and very low concentrations are sufficient to bind to TetR. In this system, expression is activated by the addition of AHT, a tetracycline derivate without antibiotic activity and a higher binding specificity to TetR as tetracycline (10^{11} M^{-1} vs. 3×10^9 M^{-1}) (Mossman, 1983; Oliva et al., 1992). Absence of AHT causes repression of the operons or genes of interest (Fig. 1). The Tet-on expression cassette can be used to replace the native promoter of gene/s under study in the natural genomic context. For this replacement, template vector p3773 is used for generation of the Tet-on cassette, and the λ Red recombineering system is used for precise targeting into the genome (Gerlach et al., 2007). For transfer of P_{tetA}-controlled genes or operons in homologous or heterologous host organisms, the fusions may be subcloned onto low copy number vectors like plasmid pWSK29 used here. *Salmonella enterica* serovar Typhimurium (STM) and *E. coli* (EC) were used as host strains.

3.2. Controlled expression of bacterial motility

We first used the Tet-on system to control expression of *fliC,* encoding the main flagella subunit flagellin. Therefore we cloned 7*fliC* of STM downstream of P_{tetA}. When we induced expression of *fliC* in STM Δ*fliC* Δ*fljB* with 100 ng/ml AHT, synthesis of FliC was detected by Western blot analysis (Fig. 2A). The deletion strain as well as the non-induced control showed no respective product. To test if AHT-induced FliC is assembled into functional flagella, we visualized STM WT, STM Δ*fliC* Δ*fljB* and STM Δ*fliC* Δ*fljB* [P_{tetA}::*fliC*] before and 3.5 h after AHT induction by microscopy (Fig. 2B). Flagellar staining was used to visualize flagella. STM Δ*fliC* Δ*fljB* and the non-induced control showed no flagella, whereas assembled flagella were detected on the induced strains harboring [P_{tetA}::*fliC*].

To elucidate if Tet-on controlled flagella are functional, we analyzed live bacteria and observed restoration of bacterial motility in AHT-induced STM Δ*fliC* Δ*fljB* [P_{tetA}::*fliC*]. The deletion mutant as well as the non-induced STM Δ*fliC* Δ*fljB* [P_{tetA}::*fliC*] showed no movement. Quantitative analyses of the bacterial motility revealed that compared to STM WT, 84% of the induced STM Δ*fliC* Δ*fljB* [P_{tetA}::*fliC*] were motile (Fig. 2D). Next, we determined motility on swim agar plate with or without addition of AHT (Fig. 2C). As control WT STM with sfGFP under Tet-on was used. GFP fluorescence was only observed on swim plate containing AHT (data not shown). While the swim zones were absent of STM Δ*fliC* Δ*fljB* and STM Δ*fliC* Δ*fljB* [P_{tetA}::*fliC*] in absence of AHT, the swim zones of STM WT, and WT [P_{tetA}::*fliC*] and Δ*fliC* Δ*fljB* [P_{tetA}::*fliC*] on plate with 100 ng/ml AHT increased from 2 to 8 h of incubation. However, extended incubation of 24 h indicated that the swim zone of STM Δ*fliC* Δ*fljB* [P_{tetA}::*fliC*] did not increase further, while motility of the WT continued.

Interestingly, the microscopic inspection of STM Δ*fliC* Δ*fljB* [P_{tetA}::*fliC*] after AHT induction revealed that only one polar flagellum was present, in contrast to the peritrichous flagellation observed for WT STM (Fig. 2B). Further quantification revealed that peritrichous flagellation was completely absent in AHT–induced STM Δ*fliC* Δ*fljB* [P_{tetA}::*fliC*] and all flagellated bacteria had only one flagellum (Fig. 2E). The formation of a single flagellum was observed at various AHT concentrations tested (10, 25, 50, or 100 ng/ml). We conclude that the Tet-on system allows control of flagella assembly and motility.

3.3. Tet-on for controlled production of fimbrial adhesins

Adhesins play an important role in the lifestyle of bacteria. They are involved in binding to biotic and abiotic surfaces, biofilm formation and dissemination of bacteria. With this system in hand, we were able to functionally express and visualize the adhesiome of STM in the non-fimbriated *E. coli* strain ORN172 (Hansmeier et al., 2017).

To further elucidate the capability of this expression system, we tested expression of Type I fimbriae (Fim), plasmid-encoded fimbriae (Pef) and Stf fimbriae (Stf) under Tet-on control in STM and in EC ORN172. The fimbriae belong to the large group of chaperone-usher fimbrial adhesins. Assembly requires secretion of subunits into periplasm and coordinated interplay of the periplasmic chaperone and outer membrane usher for the assembly of polymeric fimbrial shafts and tip adhesins (Hospenthal et al., 2017). Synthesis and surface expression of fimbriae in EC ORN172 and STM Δ*fim* was analyzed by Western blotting and flow cytometry, respectively (Fig. 3AB). When we induced expression of *fim*, *stf*, or *pef* fimbriae with 100 ng/ml AHT in EC or STM, we detected expression of the respective main fimbrial subunits by Western blotting, while no bands were detectable in negative controls or non-induced samples. Surface expression of fimbriae was determined by flow cytometry. In all cases, we detected populations of bacteria with increased fluorescence signals in induced samples compared to non-induced samples or negative controls, indicating that fimbriae were successfully expressed on the surface of the bacteria. Percentages of bacteria expressing fimbriae in EC ranged from 22% for

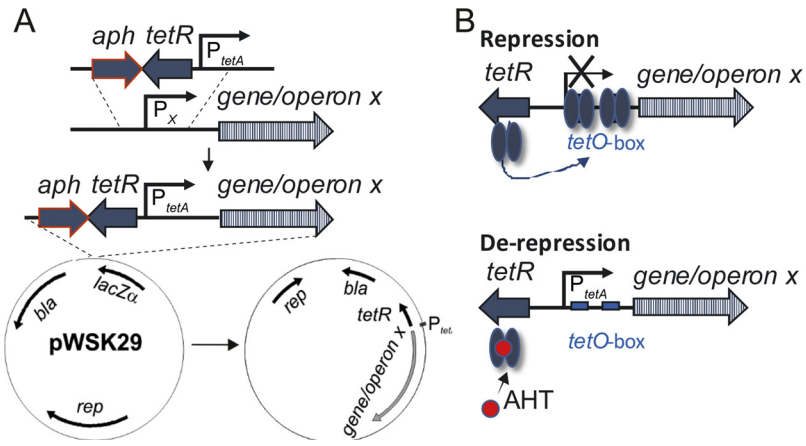

Fig. 1. Scheme for inducible expression of secretion systems, autotransporter adhesins or T3SS substrate proteins. **A**. For controlled expression, promoters of genes or operons of interest were replaced by a tetracycline-inducible expression cassette, containing the Tet repressor *tetR*, the *tetA* operator (promoter of the tetracycline-exporter TetA and *tetO* boxes) and, for selection, *aph* encoding the aminoglycoside 3-*N*-acetyltransferase conferring kanamycin resistance. For plasmid-borne expression, this tetracycline-inducible expression cassette with operons or genes of interest was introduced into pWSK29. **B.** In absence of tetracycline or derivatives such as doxycycline or anhydrotetracycline (AHT), Tet repressor protein (TetR) binds as a homodimer to operators *tetO* boxes and blocks transcription of the operons or genes of interest. In contrast, in presence of AHT, TetR dissociates from *tetO* and transcription of the operons or genes of interest is initiated.

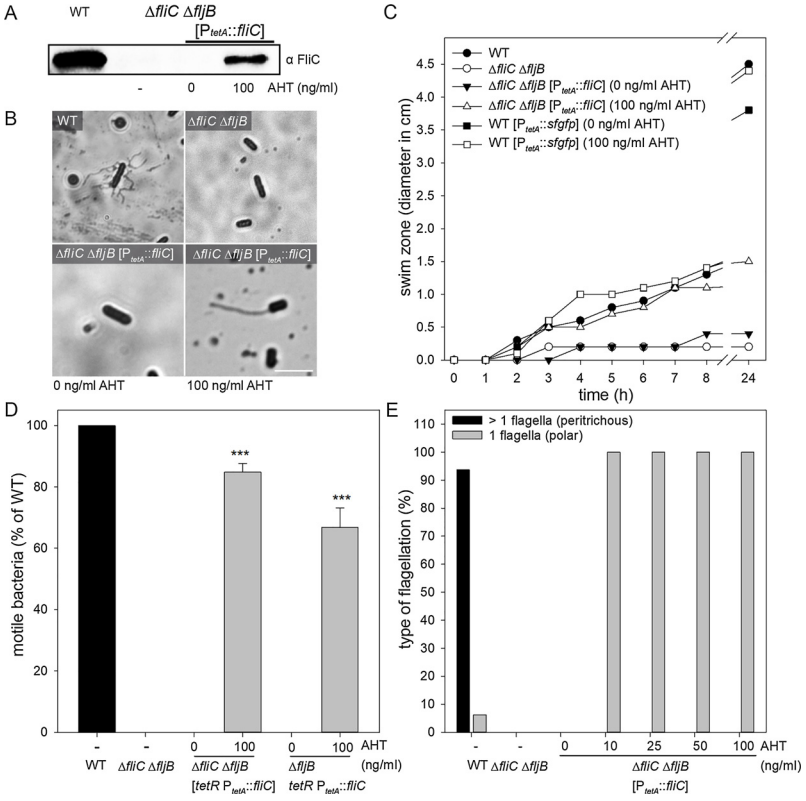

Fig. 2. Inducible flagellar assembly and motility. STM Δ*fliC* Δ*fljB* harboring the expression plasmid for *fliC*, and STM WT and STM Δ*fliC* Δ*fljB* as positive and negative controls, respectively, were grown aerobically for 3.5 h in presence or absence of 100 ng/ml AHT. **A.** Expression of the major flagellar subunit FliC was analyzed by Western blots of lysates of STM WT and after AHT induction in STM Δ*fliC* Δ*fljB* [P_{tetA}::*fliC*] using *Salmonella* O-antigen-specific antibody. For loading control, see **Fig. S 1**. **B.**Flagella were visualized with flagella stain (BD), and micrographs of respective STM strains show presence (WT), absence (D*fliCDfljB*) and reinstatement of flagella (D*fliCDfljB*[P_{tetA}::*fliC*]) after AHT induction. Scale bar, 2 µm. **C.** STM WT,D*fliCDfljB* without or with[P_{tetA}::*fliC*], and WT [P_{tetA}::*sfgfp*] were inoculated in the center of swim agar plates without or with 100 ng/ml AHT as indicated. Plates were incubated at 30°C and diameters of swim zones were determined in hourly intervals. **D**. Restoration of flagellar motility in STMD*fliCDfljB*[P_{tetA}::*fliC*] after AHT induction. Indicated STM strains were grown aerobically in absence or presence of AHT for 3.5 h and cellular motility was quantified by microscopic inspection of at least 100 bacteria per strain. The proportion of the motile bacteria is given as percentage of STM WT set to 100 %. Statistical analysis was performed by One-way ANOVA. ***, $P < 0.001$. **E**. Flagella staining was performed as for Δ, and at least 100 bacterial cells per strain/condition were scored for presence of single, polar or multiple, peritrichous flagella. Various concentrations of AHT as indicated were used for induction of *fliC* expression in STMD*fliCDfljB*[P_{tetA}::*fliC*]..

Pef fimbriae to 79% for Fim and Stf fimbriae, which are similar levels as in STM. We visualized the chaperone-usher fimbriae on the surface of EC and STM by atomic force microscopy (AFM) and observed comparable morphologies (Fig. 3C). The diameters of the fimbriae were in similar ranges when expressed in STM or EC (data not shown).

We investigated the scalability of Tet-on expression comparing Tet-on controlled chromosomal *pef* in STM (STM P_{tet}::*pef*), or ectopically on the low copy-number plasmid pWSK29 in a STM Δ*pef* strain (STM Δ*pef* [P_{tet}::*pef*]), or in EC [P_{tetA}::*pef*] (Fig. S 2). With increasing concentrations of AHT, we detected expression of the main subunit PefA by Western blotting starting at 2.5 ng/ml AHT under all conditions (Fig. S 2A, C, E). Increased AHT concentrations up to 25 ng/ml resulted in increased amounts of PefA. Surface expression of Pef fimbriae was determined by flow cytometry (Fig. S 2B, D, F). When we induced expression of Pef fimbriae ectopically expressed in STM Δ*pef* [P_{tetA}::*pef*] or in EC [P_{tetA}::*pef*], we detected expression of Pef fimbriae starting with 1 ng/ml AHT, while maximal expression was reached with 25 ng/ml AHT. Surface expression of PefA in STM P_{tetA}::*pef* was detectable after induction with 1 ng/ml AHT. However, quite surprisingly, maximal surface expression was reached after induction with 5 ng/ml AHT, while decreasing with higher concentrations of AHT (Fig. S 2). High amounts of assembled Pef fimbria may lead to altered properties of bacteria in flow cytometry, thus preventing detection. Alternatively, levels of *pef* expression too high could perturb proper assembly of fimbriae on the bacterial surface.

The kinetics of expression was analyzed using STM with Tet-on control of the chromosomal *fim* operon, or plasmid with Tet-on control of the *fim* operon in STM Δ*fim* or EC Δ*fim* (Fig. 4). Cultures were induced by addition of a fixed concentration of 100 ng/ml AHT, and at various time points after induction, aliquots of cultures were analyzed for amounts of main subunit FimA by Western blot (Fig. 4A, C, E) and Fim surface expression by flow cytometry (Fig. 4B, D, F). We detected FimA already 10 min after addition of AHT in Western blots, and STM positive for surface expression of Fim fimbriae emerged after 10 min. The proportion of the Fim-positive cells rapidly increased, reaching a maximum of 40% Fim-positive STM cells 25 min after induction for

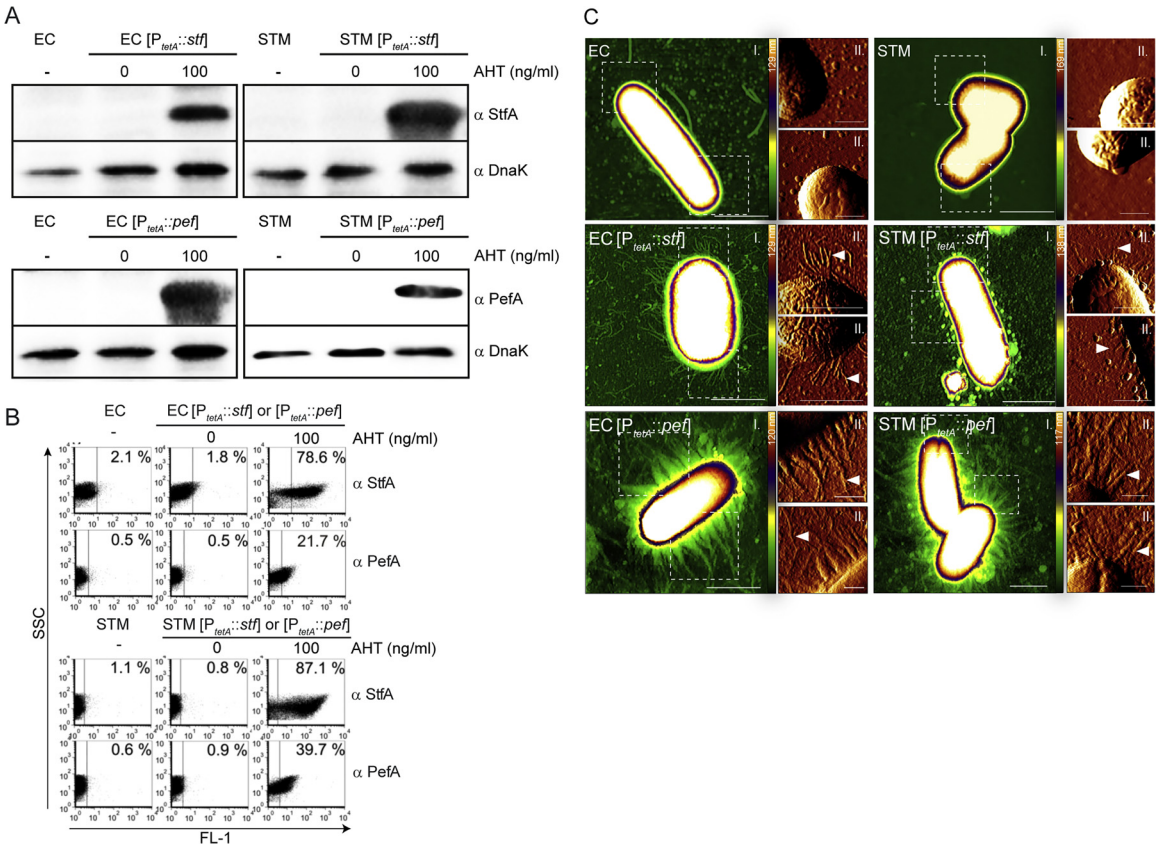

Fig. 3. Controlled synthesis and surface expression of chaperone-usher fimbrial adhesins in *E. coli* or *Salmonella*. Fimbrial operons *stfACDEFGH* or *pefACDEF* of STM were placed under control of the Tet-on expression cassette on pWSK29 and transferred in EC ORN172 or STM WT. STM and EC and strains were grown in a roller drum for 3.5 h in absence or presence of 100 ng/ml AHT. **A.** Synthesis of main fimbrial subunits StfA or PefA was detected by Western blotting from lysates of respective EC and STM strains. As loading controls, blots were stripped and reprobed with antibody against DnaK. **B.** Surface expression of fimbriae in indicated strains was assessed by flow cytometry based on detection of the main subunits StfA or PefA. The percentage cells positive for StfA or PefA surface expression is indicated. **C.** Fimbrial adhesins expressed in STM or EC ORN172 were visualized by AFM. Each panel contains an AFM height image (I), and enlarged deflection images (II). Arrow heads point to the respective adhesive structure in the deflection images. Scale bars indicate 1 µm (I) or 0.5 µm (II). (For interpretation of the references to colour in this figure legend, the reader is referred to the web version of this article).

chromosomal Tet-on *fim* (Fig. 4B). For episomal Tet-on *fim*, a maximum of 53% Fim-positive STM was already reached 15 min after induction (Fig. 4D). FimA synthesis and surface expression of Fim fimbriae in EC was delayed compared to STM (Fig. 4E, F). In contrast, under native control expression of Fim fimbriae was detected in about 10% of STM WT cells after 24 h incubation as standing cultures (Fig. 4G). Our results indicate that the Tet-on system allows efficient and rapid synthesis and assembly of complex, multimeric surface structures. Our prior work also indicated adhesin function of Tet-on-controlled Fim and Curli fimbriae, T1SS-secreted BapA, and non-fimbrial adhesins MisL and ShdA of STM (Hansmeier et al., 2017).

3.4. AHT-inducible synthesis and surface expression of autotransporter adhesins

Next, we tested the Tet-on expression system for autotransported adhesins in heterologous hosts. Autotransporter adhesins are important virulence factors in Gram-negative pathogens and a simple form of non-fimbrial adhesins consisting of one protein subunit (Lyskowski et al., 2011; Pepe and Miller, 1990). We cloned genes encoding autotransporter Inv or trimeric autotransporter YadA of *Y. enterocolitica* under control of P_{tetA}. After induction of YadA or Inv in EC ORN172 with addition of 100 ng/ml AHT (Fig. 5A), bands of the molecular weight of YadA or Inv were detected, which were absent in non-induced controls or in bacteria which did not contain the respective expression constructs. Using flow cytometry we detected increased fluorescence signals after induction of expression of *inv* or *yadA* compared to non-induced controls (Fig. 5B). If STM was used as heterologous host for expression of *Y. enterocolitica* autotransporter adhesins, we observed similar specificity of induction by AHT (Fig. S 3). These results indicate that both YadA and Inv were successfully autotransported and assembled on bacterial surfaces.

We visualized YadA and Inv by transmission electron microscopy (TEM). On the surface of *E. coli* expressing YadA, pin-like structures were visible which were not present in non-induced controls (Fig. 5C). These structures resembled previously published TEM images of YadA (Hoiczyk et al., 2000). To further scrutinize the identity of the surface structures, immunogold-labelling was performed. Specific labeling by gold-particles was observed, which was not present in non-induced controls (Fig. 5C). These results confirm the functional expression of YadA and Inv.

3.5. AHT-inducible synthesis and surface expression of EHEC adhesins

Enteropathogenic *E. coli* (EHEC) are highly pathogenic EC strains. Recent outbreaks of fresh produce-associated EHEC infections gave rise to increased interest in understanding of transmission of this pathogen along the food chain. As for STM, the genome of EHEC strains encodes a large number of known or putative fimbrial and non-fimbrial adhesins (McWilliams and Torres, 2014). Since biological safety requirements limit the direct experimental analysis of adhesin function in EHEC, we considered the Tet-on approach as a useful alternative. As candidate

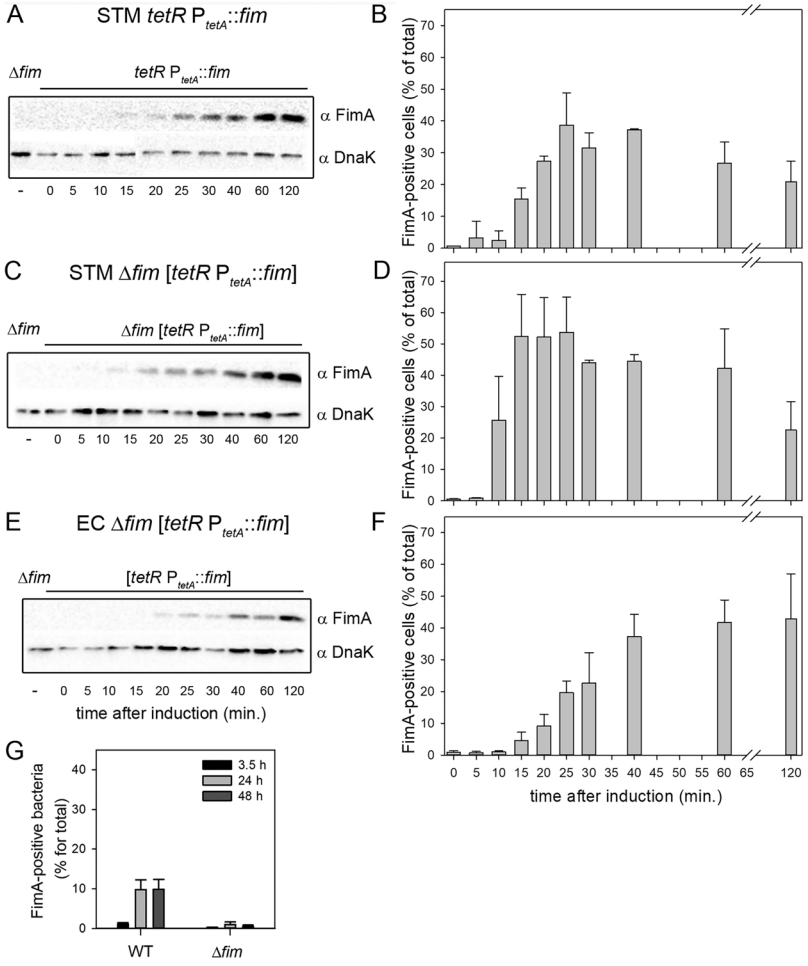

Fig. 4. Kinetics of AHT-induced synthesis of FimA and surface expression of Fim fimbriae. The promoter of the chromosomal *fim* operon in STM was replaced by the Tet-on cassette (**A, B**), or the *fim* operon downstream of the Tet-on cassette was cloned in vector pWSK29 and the resulting plasmid was introduced in an STM Δ*fim* strain (**C, D**) or EC Δ*fim* strain ORN172 (**E, F**). Cultures were grown with aeration at 37 °C in a roller drum and induced by addition of AHT to a final concentration of 100 ng/ml if indicated. **G**) STM WT and STM Δ*fim* were cultured in LB broth for 3.5 h with agitation in a roller drum, or for 24 or 48 h as standing culture. Culture aliquots were collected prior and at various time points after AHT addition and processed for Western blot analyses of FimA and DnaK as loading control **(A, C, E)**, or flow cytometry for determination of FimA-positive bacteria (**B, D, F, G**). The percentage of cells positive for Fim surface expression is given, and means and standard deviations of three independent experiments are shown.

adhesin, we selected the chaperone-usher (C/U) adhesin *E. coli* Common Pilus (ECP), that is involved in adhesion to mammalian epithelial cells (Rendon et al., 2007) and recently was demonstrated to mediate adhesion to plant surfaces (Rossez et al., 2014). The ECP operon of outbreak strain EHEC O157:H7 Sakai was cloned in a Tet-on vector and expressed in an EC laboratory strain and STM (Fig. 6). As for STM fimbriae, we observed efficient induction of main subunit EcpA (Fig. 6A), surface expression of ECP in both heterologous hosts, and 50% or 40% of EC or STM cells were positive for surface expression of ECP (Fig. 6B). Visualization by AFM or TEM revealed that ECP expressing EC or STM were decorated with large number of the ECP appendages if expression was induced (Fig. 6CD, 100 ng/ml AHT), while surface appendages were absent in non-induced controls (Fig. 6CD, 0 ng/ml AHT). The length and morphology of heterologous expressed ECP was comparable to ECP on the surface of pathogenic EC stains (Rendon et al., 2007). We also succeeded to functionally express various other fimbrial and non-fimbrial adhesins of EHEC O157:H7 outbreak strain Sakai and EAEC outbreak strain O104:H4 C227 (L.E., unpublished observations). We conclude that the Tet-on system provides an efficient and robust experimental tool for structural and functional characterization of adhesins of highly pathogenic bacteria.

3.6. Tet-on for controlled secretion and translocation of type III secretion system substrate proteins

The bacterial type III secretion systems (T3SS) and their repertoires of translocated proteins are key elements in diseases caused by Gram-negative bacteria pathogenic to plants, animals or man. Translocation of effector proteins of the *Salmonella* Pathogenicity Island 2 (SPI2)-encoded T3SS by intracellular STM leads to massive remodeling of the host cell endosomal system and *Salmonella*-induced filaments (SIF) are a prominent phenotypic consequence (Liss and Hensel, 2015). STM strains deficient in SifA fail to induce SIF, while mutant strains defective in SseF and/or SseG induce SIF with aberrant morphology termed 'pseudo-SIF' (Kuhle and Hensel, 2002). Both phenotypes are distinct and easily distinguishable from the SIF morphology induced by STM WT. Thus, we selected effector proteins SifA, SseF and SseG as candidates for Tet-on controlled expression.

We generated epitope-tagged alleles of single effector *sifA*::M45 or combination of two effectors *sseF*::HA *sseG*::M45 under control of P_{tetA} in pWSK29. The resulting vectors were introduced in STM WT and the respective deletion strains. Western blot analyses confirmed the synthesis of all effectors after induction with 100 ng/ml AHT (Fig. 7AB). Synthesis of the effector proteins was absent in non-induced controls. Next, we analyzed if effector proteins synthesized under control of the Tet-on system are also translocated into host cells (Fig. 7CD). STM harboring plasmids [*sifA*::M45] or [*sseF*::HA *sseG*::M45] with effector genes under control of their native promoters were used as positive controls, as their expression were already described elsewhere (Halici et al., 2008; Hansen-Wester et al., 2002; Kuhle and Hensel, 2002). We infected epithelial cell line HeLa stably expressing LAMP1-eGFP (Krieger et al., 2014) with STM [P_{tetA}::*sifA*::M45] or [P_{tetA}::*sseF*::HA *sseG*::M45] as well as the respective control strains STM [*sifA*::M45] or [*sseF*::HA *sseG*::M45]. At 3 h p.i. STM [P_{tetA}::*sifA*::M45] or STM [P_{tetA}::*sseF*::HA *sseG*::M45] were left non-induced (0 ng/ml AHT) or induced (100 ng/ml AHT). Cells were fixed and immuno-stained against *Salmonella* O-antigen and the respective epitope tags (HA or M45) for visualization by epifluorescence microscopy.

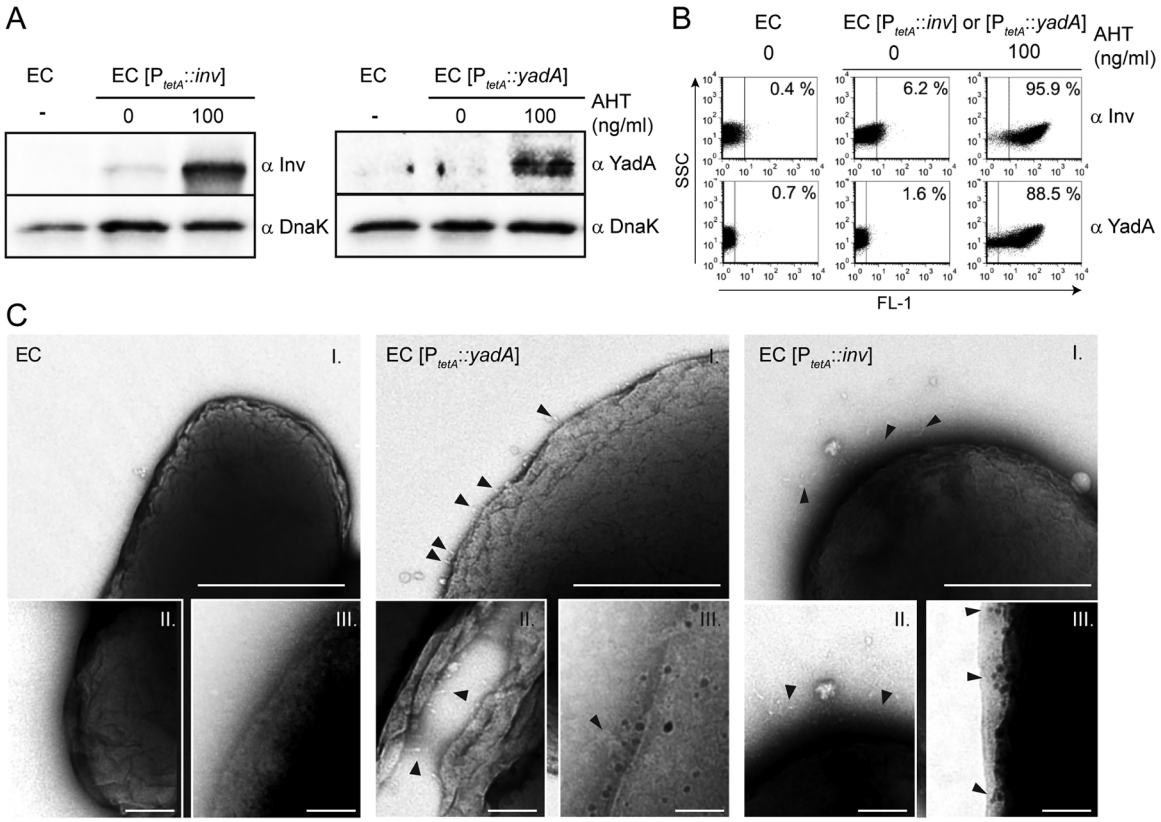

Fig. 5. Synthesis and surface expression of autotransporter adhesins of *Yersinia enterocolitica* in *E. coli* ORN172. *Yersinia enterocolitica inv* or *yadA* were cloned on plasmids under control of the Tet-on cassette and resulting plasmids were introduced into EC ORN172. Strains without plasmid (negative control), or harboring the indicated expression plasmid were grown for 3.5 h aerobically in presence or absence of 100 ng/ml AHT. **A.** Synthesis of Inv and YadA under control of the Tet-on cassette was analyzed by Western blotting using antisera specific to the respective adhesin. As loading controls, blots were stripped and reprobed with antibody against DnaK. **B.** Surface presentation of autotransporter adhesins by EC was detected by flow cytometry of fixed cell with adhesin-specific antisera. Immuno-labeled EC without plasmid were used to define gating. The percentage of Inv- or YadA-positive cells is indicated. **C.** Visualization of autotransporter adhesins on EC by TEM after negative staining. Each panel contains an overview image (I), and enlarged unstained (II) and immuno-gold labeled TEM images (III). Arrow heads point to the respective surface structures. Scale bars indicate 0.5 µm (I) or 0.1 µm (II).

At 8 h p.i., we observed translocation of SifA-M45, SseF-HA and SseG-M45 infected cells and co-localization with LAMP1 along SIF after AHT induction, whereas the non-induced strains showed no effector translocation (Fig. 7CD). Effector proteins synthesized under control of their native promoters and under control of the Tet-on system showed similar subcellular distribution, LAMP1 co-localization, and decoration of SIF membranes. Thus, there is no visual difference between Tet-on induction and native controlled effector expression.

The additional metabolic burden of ectopic expression of virulence factors and the absence of antibiotic selection of plasmids under *in vivo* conditions may force the loss of plasmids and by this reduce the efficiency of the Tet-on systems. To account for this potential artifact, we tested the stability of representative Tet-on plasmids for expression of the *pef* operon, or effector proteins of the SPI2-T3SS (Fig. S 4). We did not observe significant loss of Tet-on plasmids after AHT induction in the absence of selective pressure under culture conditions, or in intracellular STM.

Next, we tested the functionality of the inducible effector expression system (Fig. 8). HeLa LAMP1-GFP cells were infected with STM WT, Δ*sifA,* or Δ*sifA* [P_{tetA}::*sifA*::M45]. Imaging was performed 8 h p.i. and the induction of SIF was analyzed in infected host cell (Fig. 8A). SIF formation was detected in more than 80% of STM WT-infected cells, but was absent in STM Δ*sifA*-infected cells. A plasmid for expression of *sifA* under control of the native promoter restored SIF formation in ca. 75% of infected cells. Tet-on expression of *sifA* also restored SIF formation, and about 35% of infected cells showed SIF (Fig. 8B). We analyzed the contribution of effector proteins SseF and SseG. Cells infected with STM Δ*sseFG* or Δ*sseFG* [P_{tetA}::*sseF*::HA *sseG*::M45] without addition of AHT showed 'pseudo-SIF' phenotype, while AHT induction of STM Δ*sseFG* [P_{tetA}::*sseF*::HA *sseG*::M45] restored normal SIF morphology in infected host cells (Fig. 8C). We quantified SIF morphologies at 0, 2, 4, and 6 h after AHT induction of *sseFG* expression (Fig. 8D). Over time of induction, the number of host cells showing pseudo-SIF continuously decreased, while the proportion of cells with normal SIF increased to more than 80% at 6 h after Tet-on induction.

Finally, we investigated if the Tet-on system can be applied to control effector synthesis and translocation in temporal precisely controlled manner in living host cells (Fig. 8E). Time-lapse microcopy was performed over 105 min and allowed tracking of individual SIF in infected cells. As expected for STM Δ*sseFG*, at 5 h p.i. we observed thin and discontinuous SIF or 'pseudo-SIF' indicated by small diameter and low fluorescence intensity of LAMP1-GFP-positive tubular compartments. Upon induction of intracellular STM Δ*sseFG* [P_{tetA}::*sseF*::HA *sseG*::M45] by AHT, onset of formation of SIF with normal morphology was obvious. We also detected conversion of pseudo-SIF to normal SIF with an increased extension of the SIF network over time of induction. Pseudo-SIF to SIF conversion frequently initiated in portions of SIF proximal to the SCV and continued towards peripheral portions (Fig. 8E).

These data show that the Tet-on system is suited to precisely control T3SS effector synthesis, subsequent translocation, and action in host cells in a live cell imaging setting.

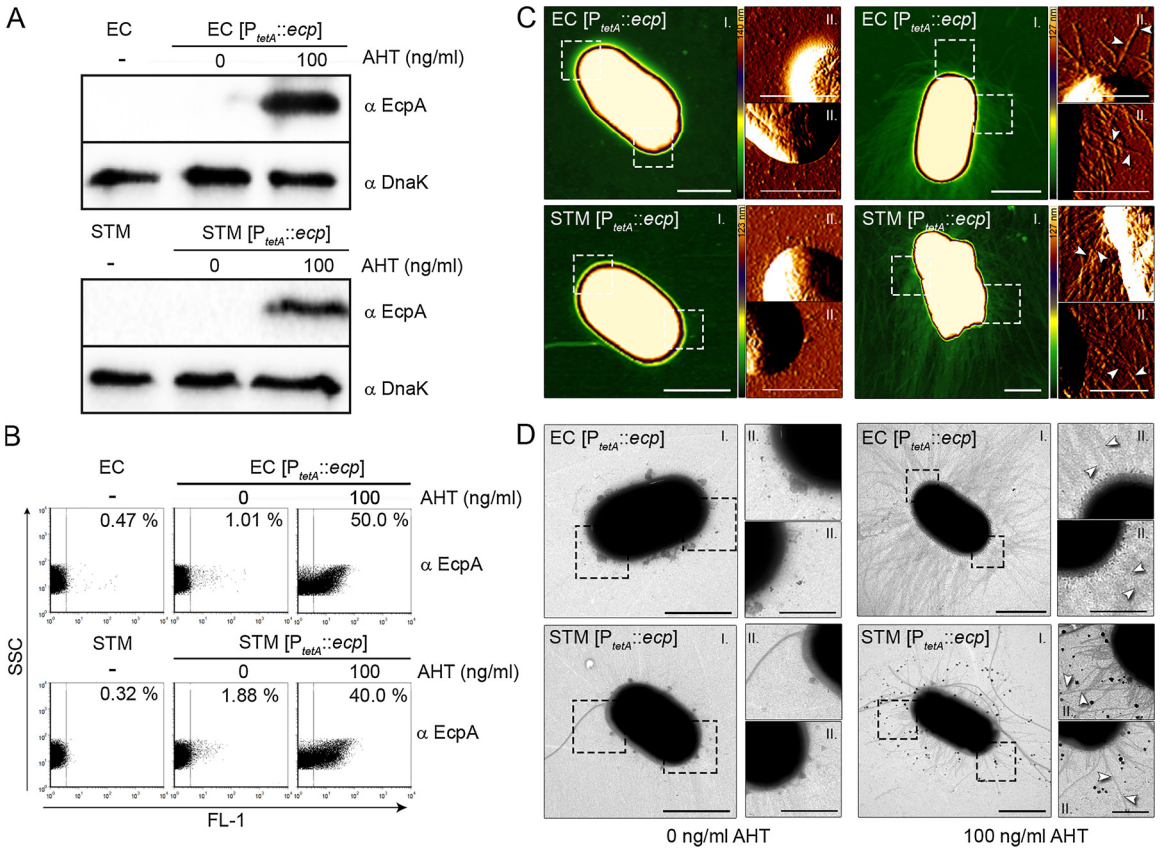

Fig. 6. Synthesis and surface expression of chaperone-usher adhesin Ecp of enteropathogenic *E. coli* in heterologous hosts. The *ecp* operon of EHEC O157:H7 strain Sakai was cloned under control of the Tet-on cassette and the resulting plasmid was introduced in EC ORN172 or STM. Strains without plasmid (negative control), or harboring the indicated expression plasmid were grown for 3.5 h aerobically in presence or absence of 100 ng/ml AHT. **A.** Synthesis of EcpA under control of the Tet-on cassette was analyzed by Western blotting using specific antisera. As loading controls, blots were stripped and reprobed with antibody against DnaK. **B.** Surface expression of Ecp fimbriae in EC or STM was detected by flow cytometry of fixed cell with antisera specific to EcpA. Immuno-labeled strains without plasmid were used to define gating. The percentage of Ecp-positive cells is indicated. **C.** Visualization of Ecp on EC or STM by AFM. Each panel contains an AFM height image (I), and enlarged deflection images (II). **D.** Visualization of Ecp on EC or STM by TEM after negative staining. Each panel contains an overview image (I), and enlarged details (II). Arrow heads point to the respective surface structure in the enlarged images. Scale bars indicate 0.5 µm (I) or 0.1 µm (II). (For interpretation of the references to colour in this figure legend, the reader is referred to the web version of this article).

4. Discussion

By using the well-characterized Tet repressor and the promoter of *tetA* resistance gene, we have deployed a simple, robust and versatile system for the controlled expression of bacterial genes. In this work, we showed that the Tet-on system can be applied to control surface expression of the flagella filament, single protein adhesins, multi-subunit polymeric fimbrial adhesins and effector proteins of T3SS.

A large body of structural and biochemical data is available on the Tet repressor and its interaction with operator sequences in P_{tetA} (Berens and Hillen, 2004; Henssler et al., 2004; Resch et al., 2008). The system is well described at the molecular level and it is also applicable in tissues as demonstrated in mammalian systems. Tet-on expression systems have been frequently used for induction of transgenes in mammalian organisms, indicated an excellent ability of inducers to penetrate tissues (Loessner et al., 2009). The application of Tet-on systems for controlled expression of transgenes in eukaryotic cells, tissues and organisms is also widely documented (reviewed in Berens and Hillen, 2004; Gossen et al., 1994). Tet-on systems for control of eukaryotic gene expression have been engineered in an opposite manner, i.e. addition of inducers cause TetR binding and transcriptional activation, while the original bacterial system is based on binding of tetracycline to TetR, resulting in binding to *tetO* and activation of transcription. Modifications of the system led to generation of the Tet-off systems, in which withdrawal of inducer activates transcription under control of P_{tetA}. Such Tet-off systems are widely used in eukaryotic expression systems and Tet-off cassettes would also be of interest for bacterial systems.

The Tet-on system allows expression control by insertion of cassettes into defined positions of the chromosome of a bacterial host, as well as in episomal elements. The Tet-on controlled functions may be transplanted into heterologous hosts, as demonstrated here by expression of EHEC fimbriae or *Yersinia* autotransporter adhesins in STM and EC laboratory strains.

It is important for analyses of virulence factors that experimentally expressed variants are structurally identical to native structures. This is especially difficult when dealing with multi-protein complexes like secretion systems, in which the expression and assembly of the individual components needs to be synchronized for functionality and structural integrity. To control structural resemblance of our expressed virulence determinants we visualized these structures by AFM or TEM. Both techniques are established to resolve biological structures with nanometer resolution (Anselmetti et al., 2007; Grin et al., 2011; Kim, 2017; Xiao and Dufrene, 2016). Using these techniques, we confirmed that Pef fimbriae of STM, Ecp fimbriae of EHEC, and YadA of *Y. enterocolitica* assembled after Tet-on induction resemble published structures (Chessa et al., 2008; Hoiczyk et al., 2000; Saldana et al., 2014). We also showed that there are no structural differences between those expressed in their natural or heterologous host *E. coli*. Thus, we conclude that in closely related species such as *E. coli*, *S. enterica* and *Y. enterocolitica,* episomal

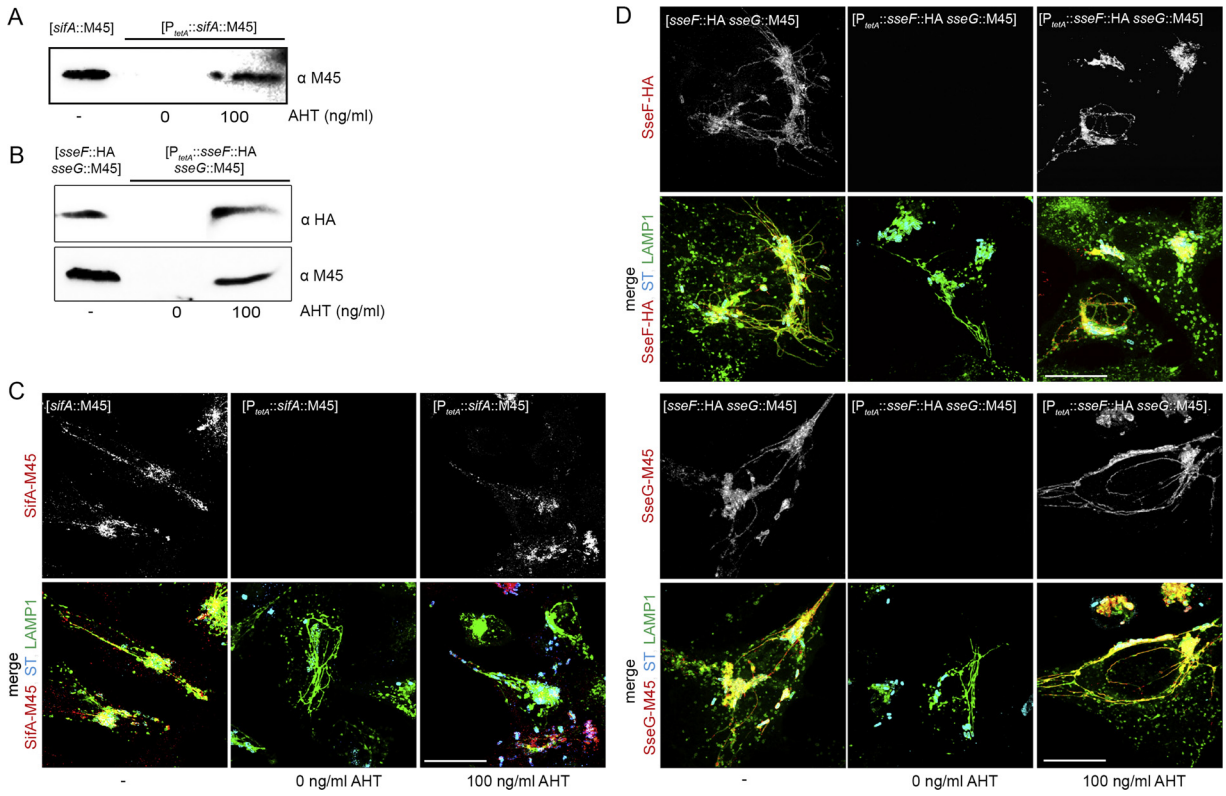

Fig. 7. Inducible synthesis and translocation of SPI2-T3SS effector proteins. Genes encoding epitope-tagged effector proteins SifA-M45 (**A, C**) or SseF-HA/SseG-M45 (**B, D**) were placed under control of native promoters, or under control of the AHT-inducible promoter. The resulting plasmids were introduced in WT STM. **A, B.** STM strains harboring the indicated expression plasmids were grown aerobically for 6 h with or without induction by 100 ng/ml AHT. Epitope-tagged effector proteins were detected by Western blots using HA- or M45-specific antibodies. Corresponding loading controls by Ponceau S staining are shown in Fig. S 1BC. **C, D.** Analysis of effector translocation in STM-infected HeLa LAMP1-GFP cells. Translocated SifA-M45 **(C)** and SseF-HA/SseG-M45 (**D**) were immuno-labeled by epitope tag-specific antibodies and visualized by CLSM. STM were visualized by *Salmonella* O-antigen staining. Overlay images are maximum intensity projections showing LAMP1 protein (green), effectors (red) and STM (turquoise). Scale bars: 20 µm. (For interpretation of the references to colour in this figure legend, the reader is referred to the web version of this article).

heterologous expression of virulence determinants is possible and that the resulting multi-protein complexes resemble their native counterpart.

In addition to the analyses of the assembly of complex polymeric surface structures in heterologous hosts, we demonstrated the control of T3SS effector synthesis and translocation. For Tet-on expression of effectors of the SPI2-T3SS there was no difference between the inducible expression of one or two effector proteins. Using the Tet-on system, we could follow the *Salmonella*-induced remodeling of the host cell endosomal system, and in particular the conversion of single membrane SIF to double membrane SIF. This phenomenon has been previously observed in host cells infected with WT STM and absent in mutant strains lacking effector proteins SseF or SseG (Krieger et al., 2014; Rajashekar et al., 2008). Here we showed that Tet-on controlled expression of *sseFG* in an *sseFG*-deficient strain leads to synthesis and translocation of the effectors, which allowed us to follow SseF/SseG-dependent remodeling in living host cells in a time-resolved manner. This on-demand expression can be instrumental for the understanding of the contribution of single or multiple effector proteins to the manipulation of host cell functions. The large number of effector proteins of T3SS and T4SS complicates the analyses of their role in host pathogen interaction. The controlled expression at a defined stage of infection, for example by intracellular STM as shown here, allows a high degree of experimental control. We observed SPI2-T3SS effector protein-dependent phenotypes in living infected host cells. This experimental option will allow to unravel the contribution of single effectors or subsets of effectors from a large group of effector proteins that are usually jointly translocated into host cells. While gene deletions cause static perturbations in host pathogen interaction, the experimentally controlled induction or repression enables investigations in dynamic systems. We initiated further studies that deploy the Tet-on system, for example, to the analysis of the role of STM adhesins with surfaces of fresh produce, to investigate the role of STM-specific peptidoglycan-modifying enzymes, or to probe the biosynthetic capacity of intracellular STM in various types of host cells (unpublished observations).

The Tet-on system can be controlled by the non-antibiotic tetracycline derivative AHT in nano-molar concentrations. AHT efficiently penetrates bacterial envelopes, and also efficiently reaches intracellular bacteria due to the efficient diffusion across membranes. Important advantages of the Tet-on system described here are the low amounts of inducer required, resulting in an inexpensive expression system, the robustness, small size of the expression cassette, and the independence from the genetic context of the host cell, thus allowing genetic transplantation for heterologous expression. Potential limitations may be the long half-life of AHT (Politi et al., 2014), sensitivity towards light of tetracycline and derivatives, and potential uncontrolled induction due to presence of trace amounts of tetracycline in materials of animal origin.

The Tet-on controlled expression is scalable by the amount of inducer applied, and the response occurs rapidly. We observed synthesis of fimbrial subunits and surface assembly of fimbriae as early as 10 min after AHT addition. This rapid response may allow new forms of analyses of the kinetics and molecular mechanisms of assembly of complex bacterial surface appendages. In contrast to other commonly used inducers for control of bacterial gene expression, AHT and other

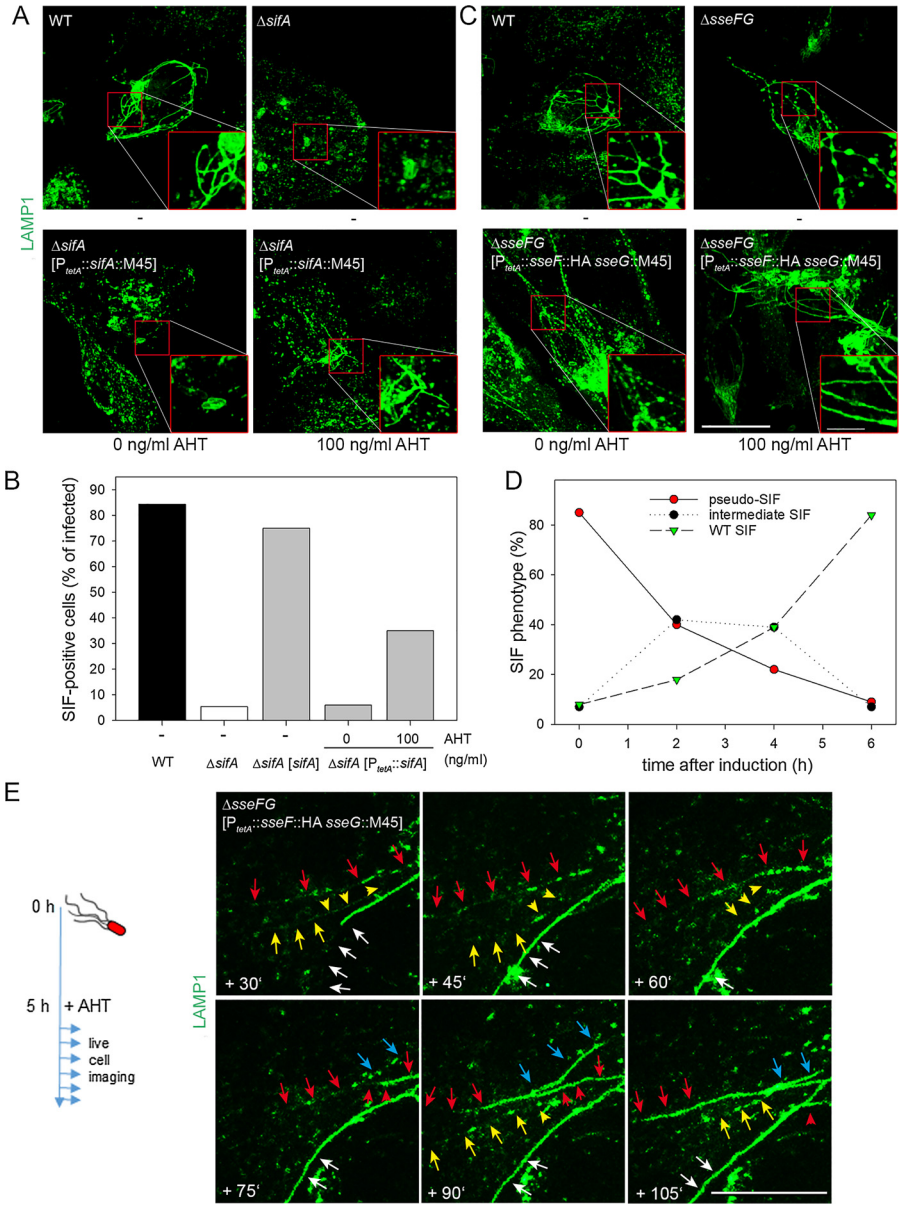

Fig. 8. Restoration of SPI2-T3SS-dependent phenotypes by Tet-on controlled effector expression. Genes encoding epitope-tagged effector proteins SifA-M45 or SseF-HA/SseG-M45 were placed under control of the AHT-inducible promoter. The resulting plasmids were introduced in STM Δ*sseFG* or Δ*sifA* strains. LAMP1-GFP (green) expressing HeLa cells were infected with STM WT, Δ*sifA*, Δ*sifA* [P_{sifA} *sifA*::M45], or [P_{tetA}::*sifA*::M45] (**A, B**), or WT, Δ*sseFG*, Δ*sseFG* [P_{tetA}::*sscB sseF*::HA *sseG*::M45] (**C, D**). If indicated, expression was induced by addition of AHT to the medium of infected host cells at 100 ng/ml final concentration. **A, C.** Representative infected cells at 8 h p.i. are shown. Scale bars: 20 µm and 5 µm in overview and details, respectively. **B.** Quantification of infected host cells showing SIF formation after infection as described for **A**. **D.** Cells were infected with STM Δ*sseFG* [P_{tetA}::*sscB sseF*::HA *sseG*::M45] as in **C**), and infected cells were scored for SIF phenotypes at various time points after AHT addition as indicated. At least 100 infected cells were investigated per strain, condition or time point (**B, D**). **E.** LAMP1-GFP (green) expressing HeLa cells were infected with Δ*sseFG* [P_{tetA}::*sscB sseF*::HA *sseG*::M45] and expression was induced by AHT addition 5 h p.i. Regions of infected host cells showing formation of tubular endosomal compartments were imaged. Red, yellow, blue and white arrows indicate the extension of individual SIF and conversion of pseudo-SIF to SIF. Time stamps indicate the time point after AHT addition in min. Scale bar: 5 µm. (For interpretation of the references to colour in this figure legend, the reader is referred to the web version of this article).

tetracycline derivatives are not metabolized and uptake does not require specific transport systems.

Tet-on systems have been used in a wide range of bacterial species, for example facultative intracellular *Listeria monocytogenes* (Schmitter et al., 2017), mycobacteria (Klotzsche et al., 2009), or obligate intracellular *Chlamydia trachomatis* (Wickstrum et al., 2013), or in tumor-targeting engineered bacteria (Kotula et al., 2014). A Tet-on system has been developed for use in *Yersinia* spp. (Obrist and Miller, 2012), and the *tetA* promoter was used to investigate the role of plasminogen-activating protease Pla of *Y. pestis* during pathogenesis of the pneumonic plaque (Lathem et al., 2007). With respect to adhesins, Tet-on systems were used for controlled expression of Ag 43 autotransporter adhesin involved in biofilm formation of *E. coli* (Da Re et al., 2007), and to investigate the contribution of Type I fimbria to formation of intracellular bacterial communities of UPEC (Wright et al., 2007). Application to bacterial protein secretion systems include use of an Tet-on control system dissect the role of the T4SS in the distinct phases of the lifecycle to intracellular *Brucella abortus* (Smith et al., 2016) and expression of T4SS subunit IcmD of the obligate intracellular pathogen *Coxiella burnetii* (Chubiz et al., 2010). A similar strategy was used by Klein et al. (2017) to investigate the role of the SPI1-encoded T3SS to control of the release of intracellular STM from the SCV. Howell et al. (2013) used a Tet-on system to control expression of T3SS effector ExoU of *Pseudomonas aeruginosa*.

To manipulate regulatory cascades, Tet-on systems were used to control expression of members of the regulatory cascade controlling genes encoding the SPI1-T3SS (Winchell et al., 2014), or the master regulator FlhDC for flagellar assembly (Sim et al., 2017). Tet-on systems are used in biotechnical protein expression systems, and form functional modules in synthetic biology approaches (Bhomkar et al., 2011; Vick et al., 2011).

To conclude, we demonstrated that the Tet-on system is a robust, versatile and broadly applicable tool for the study of complex bacterial virulence factors.

Author contributions

M.H., N.H. and T.S. designed research; N.H., K.M., L.E., M.S. and T.S. performed research; N.H., K.M., M.S. and T.S. analyzed data; and M.H, and N.H. wrote the paper with input from all authors.

Competing financial interests

The authors declare no competing financial interests.

Acknowledgements

This work was supported by the Deutsche Forschungsgemeinschaft though grants P4 and Z within collaborative research center SFB944 (to M.H.) and STE 1921/3-1 (to T.S.). Further support by a startup grant of the Ministerium für Wissenschaft und Kultur Lower Saxony to M.H. is kindly acknowledged. T.S. and N.H. received Incentive Awards for the School of Biology/Chemistry. We kindly acknowledge the excellent technical support by Monika Nietschke, Ursula Krehe, Timo Herrenkind and Luca Wallach. We like to thank Andreas Bäumler for sharing antisera against fimbrial subunits, Jorge A. Girón for antisera against EcpA, Ingo Autenrieth for YadA and Inv antisera, and Marc Erhardt for sharing antisera against FliC. The authors have declared no conflict of interests.

Appendix A. Supplementary data

Supplementary material related to this article can be found, in the online version, at doi:https://doi.org/10.1016/j.ijmm.2018.11.001.

References

Andersson, D.I., Hughes, D., 2010. Antibiotic resistance and its cost: is it possible to reverse resistance? Nat. Rev. Microbiol. 8, 260–271.
Anselmetti, D., Hansmeier, N., Kalinowski, J., Martini, J., Merkle, T., Palmisano, R., Ros, R., Schmied, K., Sischka, A., Toensing, K., 2007. Analysis of subcellular surface structure, function and dynamics. Anal. Bioanal. Chem. 387, 83–89.
Berens, C., Hillen, W., 2004. Gene regulation by tetracyclines. Genet. Eng. (N. Y.) 26, 255–277.
Bhomkar, P., Materi, W., Wishart, D.S., 2011. The bacterial nanorecorder: engineering *E. coli* to function as a chemical recording device. PLoS One 6, e27559.
Burstein, D., Zusman, T., Degtyar, E., Viner, R., Segal, G., Pupko, T., 2009. Genome-scale identification of *Legionella pneumophila* effectors using a machine learning approach. PLoS Pathog. 5, e1000508.
Chakravortty, D., Hansen-Wester, I., Hensel, M., 2002. *Salmonella* pathogenicity island 2 mediates protection of intracellular *Salmonella* from reactive nitrogen intermediates. J. Exp. Med. 195, 1155–1166.
Chessa, D., Dorsey, C.W., Winter, M., Bäumler, A.J., 2008. Binding specificity of *Salmonella* plasmid-encoded fimbriae assessed by glycomics. J. Biol. Chem. 283, 8118–8124.
Chubiz, J.E., Golubeva, Y.A., Lin, D., Miller, L.D., Slauch, J.M., 2010. FliZ regulates expression of the *Salmonella* pathogenicity island 1 invasion locus by controlling HilD protein activity in *Salmonella enterica* serovar typhimurium. J. Bacteriol. 192, 6261–6270.
Da Re, S., Le Quere, B., Ghigo, J.M., Beloin, C., 2007. Tight modulation of *Escherichia coli* bacterial biofilm formation through controlled expression of adhesion factors. Appl. Environ. Microbiol. 73, 3391–3403.
Gerlach, R.G., Holzer, S.U., Jackel, D., Hensel, M., 2007. Rapid engineering of bacterial reporter gene fusions by using Red recombination. Appl. Environ. Microbiol. 73, 4234–4242.
Gossen, M., Bonin, A.L., Freundlieb, S., Bujard, H., 1994. Inducible gene expression systems for higher eukaryotic cells. Curr. Opin. Biotechnol. 5, 516–520.
Gossen, M., Bujard, H., 1992. Tight control of gene expression in mammalian cells by tetracycline-responsive promoters. Proc. Natl. Acad. Sci. U. S. A. 89, 5547–5551.
Grin, I., Schwarz, H., Linke, D., 2011. Electron microscopy techniques to study bacterial adhesion. Adv. Exp. Med. Biol. 715, 257–269.
Halici, S., Zenk, S.F., Jantsch, J., Hensel, M., 2008. Functional analysis of the *Salmonella* pathogenicity island 2-mediated inhibition of antigen presentation in dendritic cells. Infect. Immun. 76, 4924–4933.
Hansen-Wester, I., Stecher, B., Hensel, M., 2002. Type III secretion of *Salmonella enterica* serovar Typhimurium translocated effectors and SseFG. Infect. Immun. 70, 1403–1409.
Hansmeier, N., Miskiewicz, K., Elpers, L., Liss, V., Hensel, M., Sterzenbach, T., 2017. Functional expression of the entire adhesiome of *Salmonella enterica* serotype Typhimurium. Sci. Rep. 7, 10326.
Henssler, E.M., Scholz, O., Lochner, S., Gmeiner, P., Hillen, W., 2004. Structure-based design of Tet repressor to optimize a new inducer specificity. Biochemistry 43, 9512–9518.
Hoiczyk, E., Roggenkamp, A., Reichenbecher, M., Lupas, A., Heesemann, J., 2000. Structure and sequence analysis of *Yersinia* YadA and *Moraxella* UspAs reveal a novel class of adhesins. EMBO J. 19, 5989–5999.
Hospenthal, M.K., Costa, T.R.D., Waksman, G., 2017. A comprehensive guide to pilus biogenesis in Gram-negative bacteria. Nat. Rev. Microbiol. 15, 365–379.
Howell, H.A., Logan, L.K., Hauser, A.R., 2013. Type III secretion of ExoU is critical during early *Pseudomonas aeruginosa* pneumonia. MBio 4, e00032–00013.
Humphries, A.D., Raffatellu, M., Winter, S., Weening, E.H., Kingsley, R.A., Droleskey, R., Zhang, S., Figueiredo, J., Khare, S., Nunes, J., Adams, L.G., Tsolis, R.M., Bäumler, A.J., 2003. The use of flow cytometry to detect expression of subunits encoded by 11 *Salmonella enterica* serotype Typhimurium fimbrial operons. Mol. Microbiol. 48, 1357–1376.
Kim, K.W., 2017. Electron microscopic observations of prokaryotic surface appendages. J. Microbiol. 55, 919–926.
Klein, J.A., Grenz, J.R., Slauch, J.M., Knodler, L.A., 2017. Controlled activity of the *Salmonella* invasion-associated injectisome reveals its intracellular role in the cytosolic population. MBio 8.
Klotzsche, M., Ehrt, S., Schnappinger, D., 2009. Improved tetracycline repressors for gene silencing in mycobacteria. Nucleic Acids Res. 37, 1778–1788.
Kotula, J.W., Kerns, S.J., Shaket, L.A., Siraj, L., Collins, J.J., Way, J.C., Silver, P.A., 2014. Programmable bacteria detect and record an environmental signal in the mammalian gut. Proc. Natl. Acad. Sci. U. S. A. 111, 4838–4843.
Krieger, V., Liebl, D., Zhang, Y., Rajashekar, R., Chlanda, P., Giesker, K., Chikkaballi, D., Hensel, M., 2014. Reorganization of the endosomal system in *Salmonella*-infected cells: the ultrastructure of *Salmonella*-induced tubular compartments. PLoS Pathog. 10, e1004374.
Kuhle, V., Hensel, M., 2002. SseF and SseG are translocated effectors of the type III secretion system of *Salmonella* pathogenicity island 2 that modulate aggregation of endosomal compartments. Cell. Microbiol. 4, 813–824.
Lathem, W.W., Price, P.A., Miller, V.L., Goldman, W.E., 2007. A plasminogen-activating protease specifically controls the development of primary pneumonic plague. Science 315, 509–513.
Leclerc, J.M., Quevillon, E.L., Houde, Y., Paranjape, K., Dozois, C.M., Daigle, F., 2016. Regulation and production of Tcf, a cable-like fimbriae from *Salmonella enterica* serovar Typhi. Microbiology 162, 777–788.
Liss, V., Hensel, M., 2015. Take the tube: remodelling of the endosomal system by intracellular Salmonella enterica. Cell. Microbiol. 17, 639–647.
Loessner, H., Leschner, S., Endmann, A., Westphal, K., Wolf, K., Kochruebe, K., Miloud, T., Altenbuchner, J., Weiss, S., 2009. Drug-inducible remote control of gene expression by probiotic *Escherichia coli* Nissle 1917 in intestine, tumor and gall bladder of mice. Microbes Infect. 11, 1097–1105.
Lyskowski, A., Leo, J.C., Goldman, A., 2011. Structure and biology of trimeric autotransporter adhesins. Adv. Exp. Med. Biol. 715, 143–158.
Malik-Kale, P., Jolly, C.E., Lathrop, S., Winfree, S., Luterbach, C., Steele-Mortimer, O., 2011. *Salmonella* - at home in the host cell. Front. Microbiol. 2, 125.
McWilliams, B.D., Torres, A.G., 2014. Enterohemorrhagic *Escherichia coli* adhesins. Microbiol. Spectr. 2.
Mossman, T., 1983. Rapid colorimetric assay for cellular growth and survival: application to proliferation and cytotoxicity assays. J. Immunol. Meth. 65, 55–63.
Obrist, M.W., Miller, V.L., 2012. Low copy expression vectors for use in *Yersinia* sp. and related organisms. Plasmid 68, 33–42.
Oliva, B., Gordon, G., McNicholas, P., Ellestad, G., Chopra, I., 1992. Evidence that tetracycline analogs whose primary target is not the bacterial ribosome cause lysis of Escherichia coli. Antimicrob. Agents Chemother. 36, 913–919.
Pepe, J.C., Miller, V.L., 1990. The *Yersinia enterocolitica inv* gene product is an outer membrane protein that shares epitopes with *Yersinia pseudotuberculosis* invasin. J. Bacteriol. 172, 3780–3789.
Politi, N., Pasotti, L., Zucca, S., Casanova, M., Micoli, G., Cusella De Angelis, M.G., Magni, P., 2014. Half-life measurements of chemical inducers for recombinant gene expression. J. Biol. Eng. 8, 5.
Rajashekar, R., Liebl, D., Seitz, A., Hensel, M., 2008. Dynamic remodeling of the endosomal system during formation of *Salmonella*-induced filaments by intracellular *Salmonella enterica*. Traffic 9, 2100–2116.
Ravishankar, S., Ambady, A., Ramu, H., Mudugal, N.V., Tunduguru, R., Anbarasu, A., Sharma, U.K., Sambandamurthy, V.K., Ramaiah, S., 2015. An IPTG inducible conditional expression system for Mycobacteria. PLoS One 10, e0134562.
Rendon, M.A., Saldana, Z., Erdem, A.L., Monteiro-Neto, V., Vazquez, A., Kaper, J.B., Puente, J.L., Giron, J.A., 2007. Commensal and pathogenic *Escherichia coli* use a common pilus adherence factor for epithelial cell colonization. Proc. Natl. Acad. Sci. U. S. A. 104, 10637–10642.
Resch, M., Striegl, H., Henssler, E.M., Sevvana, M., Egerer-Sieber, C., Schiltz, E., Hillen, W., Muller, Y.A., 2008. A protein functional leap: how a single mutation reverses the function of the transcription regulator TetR. Nucleic Acids Res. 36, 4390–4401.
Rosano, G.L., Ceccarelli, E.A., 2014. Recombinant protein expression in *Escherichia coli*: advances and challenges. Front. Microbiol. 5, 172.
Rossez, Y., Holmes, A., Lodberg-Pedersen, H., Birse, L., Marshall, J., Willats, W.G., Toth, I.K., Holden, N.J., 2014. *Escherichia coli* common pilus (ECP) targets arabinosyl residues in plant cell walls to mediate adhesion to fresh produce plants. J. Biol. Chem. 289, 34349–34365.
Saldana, Z., De la Cruz, M.A., Carrillo-Casas, E.M., Duran, L., Zhang, Y., Hernandez-Castro, R., Puente, J.L., Daaka, Y., Giron, J.A., 2014. Production of the *Escherichia coli* common pilus by uropathogenic *E. Coli* is associated with adherence to HeLa and HTB-4 cells and invasion of mouse bladder urothelium. PLoS One 9, e101200.
Schmitter, S., Fieseler, L., Klumpp, J., Bertram, R., Loessner, M.J., 2017. TetR-dependent gene regulation in intracellular *Listeria monocytogenes* demonstrates the spatiotemporal surface distribution of ActA. Mol. Microbiol. 105, 413–425.
Sim, M., Koirala, S., Picton, D., Strahl, H., Hoskisson, P.A., Rao, C.V., Gillespie, C.S., Aldridge, P.D., 2017. Growth rate control of flagellar assembly in *Escherichia coli* strain RP437. Sci. Rep. 7, 41189.
Smith, E.P., Miller, C.N., Child, R., Cundiff, J.A., Celli, J., 2016. Postreplication roles of the *Brucella* VirB type IV secretion system uncovered via conditional expression of the VirB11 ATPase. MBio 7.

Tobe, T., Beatson, S.A., Taniguchi, H., Abe, H., Bailey, C.M., Fivian, A., Younis, R., Matthews, S., Marches, O., Frankel, G., Hayashi, T., Pallen, M.J., 2006. An extensive repertoire of type III secretion effectors in *Escherichia coli* O157 and the role of lambdoid phages in their dissemination. Proc. Natl. Acad. Sci. U. S. A. 103, 14941–14946.

Vick, J.E., Johnson, E.T., Choudhary, S., Bloch, S.E., Lopez-Gallego, F., Srivastava, P., Tikh, I.B., Wawrzyn, G.T., Schmidt-Dannert, C., 2011. Optimized compatible set of BioBrick vectors for metabolic pathway engineering. Appl. Microbiol. Biotechnol. 92, 1275–1286.

Vorwerk, S., Krieger, V., Deiwick, J., Hensel, M., Hansmeier, N., 2015. Proteomes of host cell membranes modified by intracellular activities of *Salmonella enterica*. Mol. Cell Proteomics 14, 81–92.

Wickstrum, J., Sammons, L.R., Restivo, K.N., Hefty, P.S., 2013. Conditional gene expression in *Chlamydia trachomatis* using the *tet* system. PLoS One 8, e76743.

Winchell, C.G., Graham, J.G., Kurten, R.C., Voth, D.E., 2014. *Coxiella burnetii* type IV secretion-dependent recruitment of macrophage autophagosomes. Infect. Immun. 82, 2229–2238.

Wright, K.J., Seed, P.C., Hultgren, S.J., 2007. Development of intracellular bacterial communities of uropathogenic *Escherichia coli* depends on type 1 pili. Cell. Microbiol. 9, 2230–2241.

Xiao, J., Dufrene, Y.F., 2016. Optical and force nanoscopy in microbiology. Nat. Microbiol. 1, 16186.